Distinct roles for the *Staphylococcus aureus* POT transporter DtpT in di/tripeptide uptake and glutathione utilisation inside human macrophages

Imran Khan[a], Sandy J MacDonald[b], Sigurbjörn Markusson[c], Callum Robson[a], Joanne L Parker[c,d], Simon Newstead[c,d], Dave Boucher[a,], Marjan Van Der Woude[e] and Gavin H Thomas[a]

[a] **Department of Biology, University of York, York, United Kingdom**
[b] **Bioscience Technology Facility, University of York, York, United Kingdom**
[c] **Department of Biochemistry, University of Oxford, Oxford, United Kingdom**
[d] **Kavli Institute of Nanoscience Discovery, University of Oxford, United Kingdom**
[e] **Hull York Medical School, University of York, York, United Kingdom**

Abstract

Peptides available in biological niches inhabited by the human pathogen *Staphylococcus aureus* serve as a rich source of amino acids required for growth and successful host colonisation. Uptake of peptides by *S. aureus* involves at least two transport systems: the POT family di/tri-peptide permease DtpT and the oligopeptide ABC transporter Opp3. Here we study the individual and combined functions of DtpT and Opp3 in enabling utilisation of 282 di-/tri-peptides via a high-throughput phenotypic screen. We reveal that many peptides can be utilised via either transporter, though DtpT appears to be the primary route of uptake for dipeptides. Intriguingly, we demonstrate a preference for Asp/Glu-containing peptides among putative DtpT substrates. To measure DtpT-mediated peptide transport directly, the protein was purified and reconstituted into proteoliposomes and active transport of diverse di- and tri-peptides was demonstrated, supporting the conclusions of the phenotypic screen. During this *in vitro* analysis, we also found that DtpT could transport the biologically prevalent tripeptide reduced glutathione (GSH). In the absence of the known glutathione transporter Gis, *dtpT* is essential for growth under conditions where GSH is supplied as the sole sulphur source, identifying DtpT as the predicted second GSH uptake system of *S. aureus*. Site-directed mutagenesis of the predicted ligand binding site of DtpT suggests GSH binds the protein vertically in a manner dependent on interactions with Gln310. Finally, we demonstrate that GSH transport is required by *S. aureus* for complete fitness during *in vitro* macrophage infection experiments, and our data suggest that GSH uptake plays a role in modulating host-pathogen interactions in these infections. Together, these data reveal important new functions for DtpT, both in the utilisation of diverse peptides for growth but also providing the first clues toward a distinct role of DtpT during intracellular infection.

Introduction

Staphylococcus aureus is a Gram-positive human bacterial pathogen associated with a broad range of different disease manifestations including skin/soft tissue infections, systemic bacteraemia, endocarditis and other invasive disease states associated with significant mortality (Tong et al., 2015). Understanding the intrinsic factors contributing to bacterial fitness, colonisation and infection in these diverse niches is essential for informing the design of novel therapeutic approaches. In order to meet their nutritional requirements during infection, bacterial pathogens such as *S. aureus* possess diverse transport proteins which allow for the selective uptake of nutrients present within the host environment. While the importance of some individual transporters in successful colonisation is well documented – particularly those implicated in the acquisition of key carbon sources, amino acids and metals (Adolf et al., 2023; Handke et al., 2018; Lehman et al., 2023; Lensmire et al., 2020) – the distinct role of many transport systems and their contributions toward infection remains understudied.

Peptides serve as an abundant source of amino acids, carbon, nitrogen and sulphur in many biological contexts and, as such, most bacterial pathogens possess one or more routes of uptake for these molecules. Bacterial peptide transporters can be broadly divided into ATP-Binding Cassette (ABC) importers and secondary active transporters belonging to the Major Facilitator Superfamily (MFS), with the latter being further divided into a small number of functionally distinct groups including the proton-dependant oligopeptide transporters, or POTs (Garai et al., 2017). ABC peptide importers are unique to prokaryotes and are capable of recognising and transporting diverse oligopeptides with high affinity, with substrates ranging from di/tri-peptides up to 35-mers (Detmers et al., 2000; Doeven et al., 2004; Hughes et al., 2022; Smith et al., 1999). In addition to their canonical role in nutrient acquisition, there are examples of these transporters contributing to diverse physiological functions including cell-wall turnover (Hughes et al., 2022; Maqbool et al., 2011) and antimicrobial peptide resistance (Ackroyd et al., 2024; Wang et al., 2016), as well as acting as sensory units for intercellular and environmental signalling networks (Slamti & Lereclus, 2019). POTs, by comparison, are found across the Tree of Life and exclusively transport di- and tri-peptides or chemically related molecules of a similar size. The importance of bacterial POTs during

infection is poorly characterised, and little is known regarding their contribution to bacterial physiology outside of their general role in nutrient uptake.

To date, there are two known promiscuous peptide transport systems which are widely distributed in Staphylococci: the ABC importer-type system $Opp3_{ABCDF}$ (or Opp3) and the di-/tri-peptide POT transporter DtpT (Yu et al., 2014). In the single elegant study comparing the roles of these two systems in *S. aureus*, Opp3 was demonstrated to be required for the transport of oligopeptides from 3 to 9 residues in length, while only DtpT was thought to be responsible for dipeptide uptake (Hiron et al., 2007). *S. aureus* also possesses an ABC importer system which is specific for the biologically prevalent tripeptide glutathione (Gis_{ABCD}, or Gis) (Lensmire et al., 2023). In addition to the aforementioned systems, different *S. aureus* strains can possess up to four additional Opp3-homologues, of which Opp1 and Opp2 are likely nickel rather than peptide transporters (Hebbeln & Eitinger, 2004; Remy et al., 2013). However, Opp4 plus one additional Opp system (ACME Opp) encoded as part of the widely disseminated arginine catabolic mobile element (Yu et al., 2014) are mostly uncharacterised and could function as additional peptide transporters.

The importance of peptide utilisation in *S. aureus* infection biology is a subject of ongoing investigation. *S. aureus* secretes an arsenal of extracellular proteases with diverse functions in host immune modulation and virulence, and these enzymes contribute to the generation of peptides within the local environment which are likely to serve as a nutrient source for the bacterium (Coulter et al., 1998; Shaw et al., 2004). Consistent with this, there is evidence that *S. aureus* senses protein-rich environments via Opp3 and responds to this stimulus via upregulation of extracellular proteases (Borezée-Durant et al., 2009; Lehman et al., 2019). Recent work has demonstrated how the *S. aureus* protease aureolysin is capable of contributing to the degradation of collagen and highlights how growth on collagen-degradation products is decreased in an Opp3-deficient mutant (Lehman et al., 2019). These observations point toward a model in which host- and bacterial-derived peptides support the growth of *S. aureus* in an Opp3-dependent manner. Conversely, loss of DtpT – but seemingly not Opp3 – leads to attenuation in several models of invasive *S. aureus* infection including intravenous infection in mice and an endocarditis model in rabbits (Coulter et al., 1998). In spite of this, the functional characterisation of DtpT to date is limited, and the molecular basis of its role in bacterial survival during infection is unknown.

Recent work has aimed to understand the molecular basis of substrate promiscuity observed in POTs and delineate the mechanistic basis of proton-coupled peptide transport in these proteins (Kotov et al., 2023; Lichtinger et al., 2024; Parker et al., 2014). Despite this work, little is known regarding the substrate preferences of these transporters and how this relates to cellular lifestyle/environment. Here, we aim to address this gap in our knowledge. We apply Phenotype Microarrays (BIOLOG) to compare the utilisation of varied di- and tri-peptides by wild-type *S. aureus* JE2 against strains with disruptions in the known peptide transporters. This approach provides novel insights into the diversity of peptides utilised via DtpT and points toward distinct amino acid preferences among DtpT substrates. Further cell-based and biochemical assays serve to both support these findings and further interrogate the specificity of the system. Finally, we extend these assays to demonstrate how DtpT also serves as a transporter for the biologically prevalent metabolite reduced glutathione (GSH) and demonstrate how glutathione transport mediated by DtpT and Gis is a determinant of bacterial survival inside human macrophages.

118 ## Results
119

120 **Phenotypic screening defines the substrate landscapes of DtpT and Opp3A**

121 In order to investigate the roles of the two known peptide transporters in *S. aureus*, we
122 generated an isogenic series of strains in the USA300-derivative strain JE2 with disruptions
123 of *dtpT* and *opp3A,* as well as a double-mutant strain. With these strains in hand, we
124 exploited the power of phenotype microarrays (PMs) as a simple high-throughput approach
125 for comparing the abilities of bacterial strains to metabolise diverse substrates as energy
126 sources, including di- and tripeptides (Biolog PM Plates 6–8). (Bochner et al., 2001; Pletzer
127 et al., 2014). Collectively, these plates allowed us to compare utilisation for 282 different
128 peptides, comprising: 246 standard dipeptides (of a possible 400), 1 hydroxyproline-
129 containing dipeptide, 7 β-bonded dipeptides, 2 γ-bonded dipeptides, 12 D-amino acid-
130 containing dipeptides and 14 tripeptides. In this assay, a given peptide is supplied as the
131 primary nitrogen source, and catabolism is measured via reduction of a redox-sensitive
132 colourimetric dye, quantified over time to produce a signal curve for each strain/peptide
133 combination. A positive metabolic signal is indicative of peptide utilisation enabled by a valid
134 route of uptake and downstream catabolic pathways, while intermediate/weak signals are
135 likely to result from poor uptake (or a complete lack thereof) or incomplete catabolism
136 following internalisation.

137 Based on the signal curves produced from our PM analysis, we could observe a series of
138 distinct utilisation patterns across our four test strains (Supplemental data SD1-4). To identify
139 commonalities in the data, we subjected the raw signal curves for each peptide to unbiased
140 cluster analysis and dimensional reduction using Uniform Manifold Approximation and
141 Projection (UMAP) (Figure 1). These analytical methods provided complementary outputs,
142 with peptides belonging to a common cluster demonstrating close spatial organisation in the
143 final UMAP plot (Figure 1A-C).

144 Visual confirmation of the clusters suggested that each encompasses a distinct pattern which
145 reflects differences in the routes of peptide utilisation (Figure 1B,D). Cluster 1 (n = 15) contains
146 peptides for which a strong metabolic signal was observed for JE2 and all three mutant
147 strains, suggesting – rather intriguingly – that neither of the two known peptide transporters
148 in *S. aureus* is required for their uptake. In contrast, utilisation of peptides in cluster 2 (n = 41)
149 was maintained in single mutant strains lacking either *dtpT* or *opp3A* but abolished in the
150 double-mutant strain, suggesting that these peptides can be transported by either of our two

systems. Clusters 3 and 4 (n = 99) both present patterns wherein utilisation is abolished for the *dtpT* mutant and the double mutant, but not the *opp3* mutant, suggesting DtpT serves as the primary route of uptake for these peptides. Collectively, these two clusters account for more than one-third of the tested peptides, with those in cluster 3 (n = 58) demonstrating a more pronounced phenotype (that is, a greater difference in signal between “positive” and “negative” utilisation) when compared to those in cluster 4 (n = 41). Such a distinction likely results from either a higher rate of internalisation by DtpT or more productive downstream catabolism following uptake for cluster 3 peptides.

The three remaining clusters contain peptides for which a weak metabolic signal was observed in the wild-type JE2 strain. Cluster 5 (n = 16) encompasses peptides for which, quite surprisingly, metabolism is permitted only in mutant strains lacking *dtpT*. While the exact mechanistic basis for this pattern is unclear, we postulate that the DtpT-mediated internalisation of these peptides may be cytotoxic under the conditions tested. However, a strong signal in the *dtpT* mutant strain suggests an alternate route of internalisation for which toxicity is not observed, perhaps due to a lower overall flux which prevents toxic over-accumulation of the peptide. The remaining peptides each gave a weak/intermediate signal or were not utilised at all or across the four strains tested here, as observed in cluster 6 (n = 58) and cluster 7 (n = 53) respectively. These phenotypic patterns suggest that the supplied peptide alone cannot be effectively utilised for cellular metabolism. We do note that the mean eAUC values recorded for cluster 6 are slightly higher than those in cluster 7 across the four strains, perhaps indicating that some peptides in cluster 6 can be utilised to produce an intermediate metabolic signal.

Notably, our analysis did not identify a cluster (nor even any individual peptides) for which the patterns of metabolism suggested that utilisation was solely dependent on Opp3, which is perhaps expected given that this system is primarily implicated in the utilisation of larger oligopeptides (n ≥ 3) (Hiron et al., 2007; Lehman et al., 2019). Taken together, our findings implicate DtpT in the utilisation of at least 140 of the peptides assessed here, with 41 of these being recognised by both peptide transport systems.

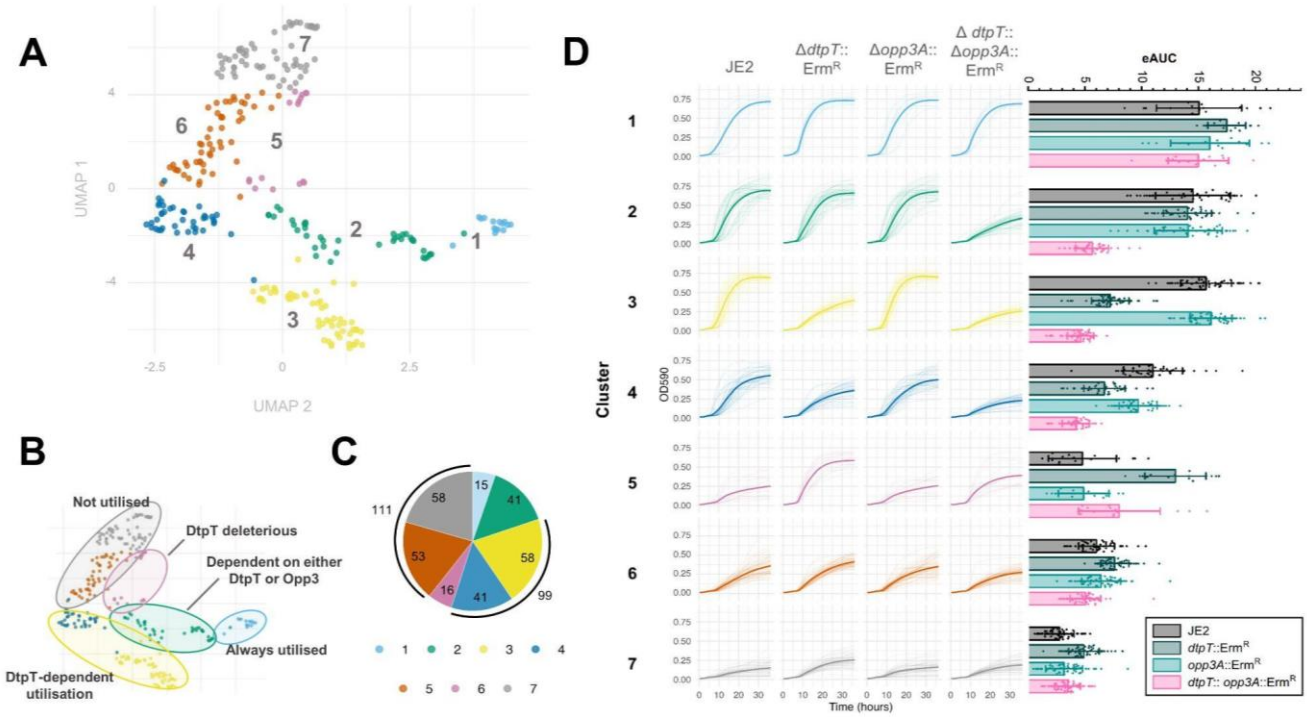

Figure 1 – UMAP and cluster analysis reveal differential peptide utilisation patterns across *dtpT* and *opp3A* mutant strains. (**A**) PM signal curves were subjected to UMAP and k-means cluster analysis (k = 7). Peptides belonging to the same cluster are grouped by colour on the UMAP plot, as labelled. (**B**) Regions of the UMAP plot corresponding to distinct phenotypic patterns (as demonstrated by cluster analysis) are highlighted. (**C**) Pie-chart representation of the number of peptides in each of the seven clusters identified here. In each case, colours correspond to the seven clusters identified in this analysis, as depicted by the key. (**D**) (**Left**) Cluster analysis reveals seven strain-specific peptide utilisation patterns. All signal curves for each cluster are overlayed and separated by strain. Mean signal curves for each strain are indicated by the bold line. (**Right**) Empirical area under the curve (eAUC) was calculated for all signal curves, as shown on the right. Bars show the mean eAUC for each strain within a given cluster. Error bars indicate standard deviation in each case.

180 **Cluster analysis demonstrates amino acid preference among putative DtpT**
181 **substrates**

182 Next, we aimed to determine whether specific amino acids were enriched within the peptides
183 of each cluster. Given the limited panel of tripeptides assessed, we focussed our analysis on
184 the 246 standard dipeptides present in the assay. First, we plotted a grid to identify potential
185 cluster-specific trends in regard to the N- and C-terminal amino acid composition of
186 dipeptides included in the phenotype microarray analysis (Figure 2). Then, we examined any
187 statistically meaningful relationships by applying a Fisher exact test (Figure 3A-D). The
188 strongest association was identified between glutamine-containing peptides and cluster 1,
189 with the vast majority (9/13) of Gln-containing peptides assessed here belonging to this
190 cluster (Figure 3A). Such an observation strongly suggests that an alternate route of uptake
191 exists for Gln-containing peptides in *S. aureus,* which is independent of both DtpT and Opp3.
192 Another clear relationship was observed between tyrosine-containing dipeptides and cluster
193 7 (Figure 3C), suggesting that tyrosine is either poorly transported or metabolised by *S.*
194 *aureus* under the conditions tested here. Tantalisingly, we observe that aspartate and
195 glutamate-containing peptides are both strongly enriched within the DtpT-specific cluster 3
196 (Figure 3D). This preference is seemingly independent of amino acid arrangement, with
197 comparable frequencies for DtpT-specific utilisation in the N- or C-terminal positions (Figure
198 2). Our findings provide compelling evidence that Asp- and Glu-containing peptides are
199 preferred transport targets for DtpT, in-turn suggesting that utilisation of these peptides is a
200 distinct function of the transporter.

201 In addition, we found that arginine-containing peptides were highly enriched in cluster 2
202 (Figure 3B), implicating both peptide transport systems in the utilisation of these peptides.
203 Arginine auxotrophy in *S. aureus* USA300 was previously demonstrated using chemically
204 defined medium containing glucose (CDMG) and the same medium lacking arginine (CDMG-
205 R) (Jeong et al., 2022; Reslane et al., 2022). Here, we exploit this auxotrophy to verify the
206 DtpT/Opp3A-dependence patterns of three arginine-containing peptides as observed in our
207 phenotypic screen. Specifically, we supplemented CDMG-R with two cluster 3 peptides (Arg-
208 Asp and Arg-Phe) and one cluster 2 peptide (Arg-Ala) and separately inoculated these media
209 with JE2 and the three mutant-derivative strains. As expected, robust growth for all strains
210 was observed in CDMG, while none of the strains were able to grow in CDMG-R (Figure 3E;
211 Figure S1A). Supplementing with Arg-Asp (cluster 3) restored growth in a completely DtpT-
212 dependent manner, while Arg-Ala (cluster 2) restored growth in all but the double mutant

213 strain (Figure 3E; Figure S1B). These patterns entirely support the findings of our phenotypic
214 screen. Unexpectedly, supplementing with Arg-Phe (cluster 3) restored growth in all but the
215 double mutant strain similarly to Arg-Ala (cluster 2). Such deviation is likely indicative of
216 differences in the sensitivity of the two approaches utilised here; that is, Opp3-mediated flux
217 of Arg-Phe is sufficient to relieve Arg auxotrophy when supplied at 1 mM, but too limited to
218 support metabolism as a sole nitrogen source under PM conditions. Finally, to further verify
219 the role of *dtpT* in the utilisation of these three peptides, we cloned the gene into a low-copy
220 number vector and were able to observe genetic complementation of growth in each case
221 (Figure S1C). Hence, we confirm that DtpT serves as a route of entry for cluster 2 and cluster
222 3 peptides, supporting the findings of our PM assays.

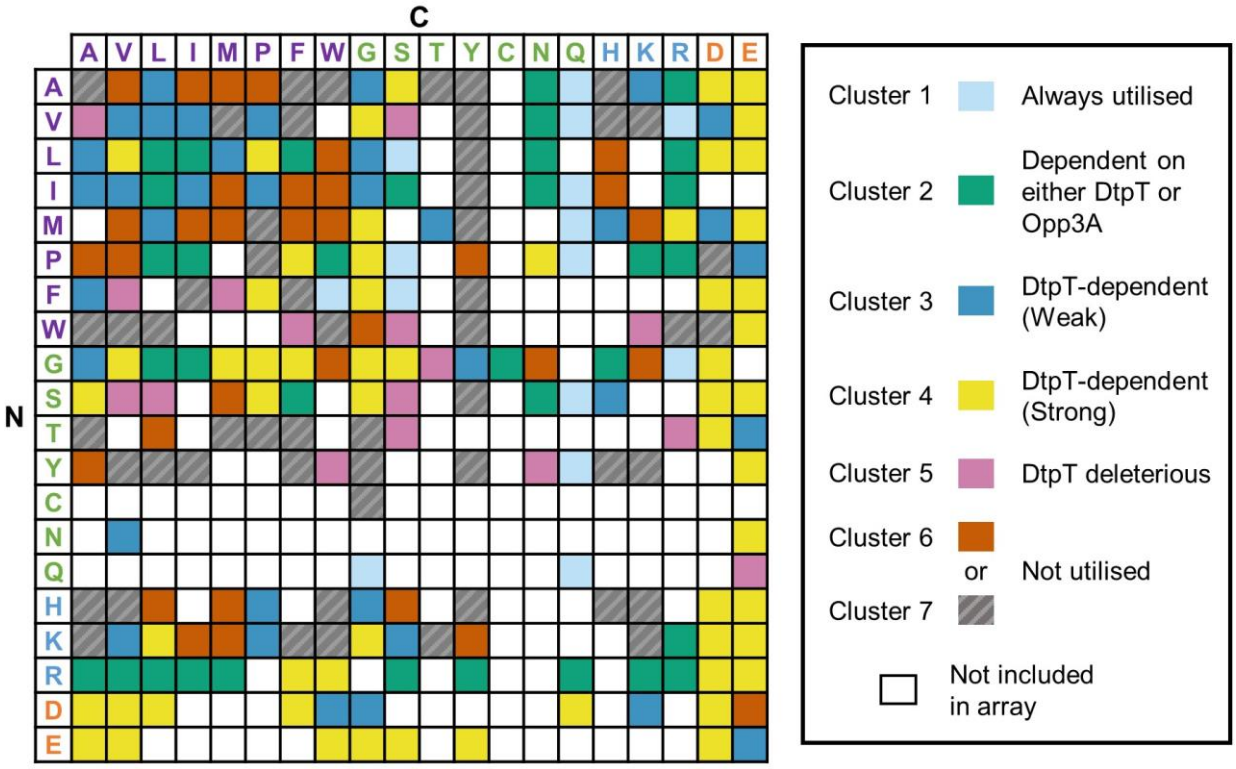

Figure 2 – Phenotype microarrays reveal differential routes of uptake for diverse dipeptides in *S. aureus.* Grid representation of all possible dipeptide structures arranged with N-terminal amino acids on the Y axis and C-terminal amino acids on the X axis. Amino acids are displayed as single-letter symbols and colour-coded according to their chemical properties (purple = hydrophobic/non-polar, green = polar/unique, blue = basic, orange = acidic). Coloured cells correspond to peptides included in the PM analysis and their corresponding utilisation patterns, as indicated by the key.

224

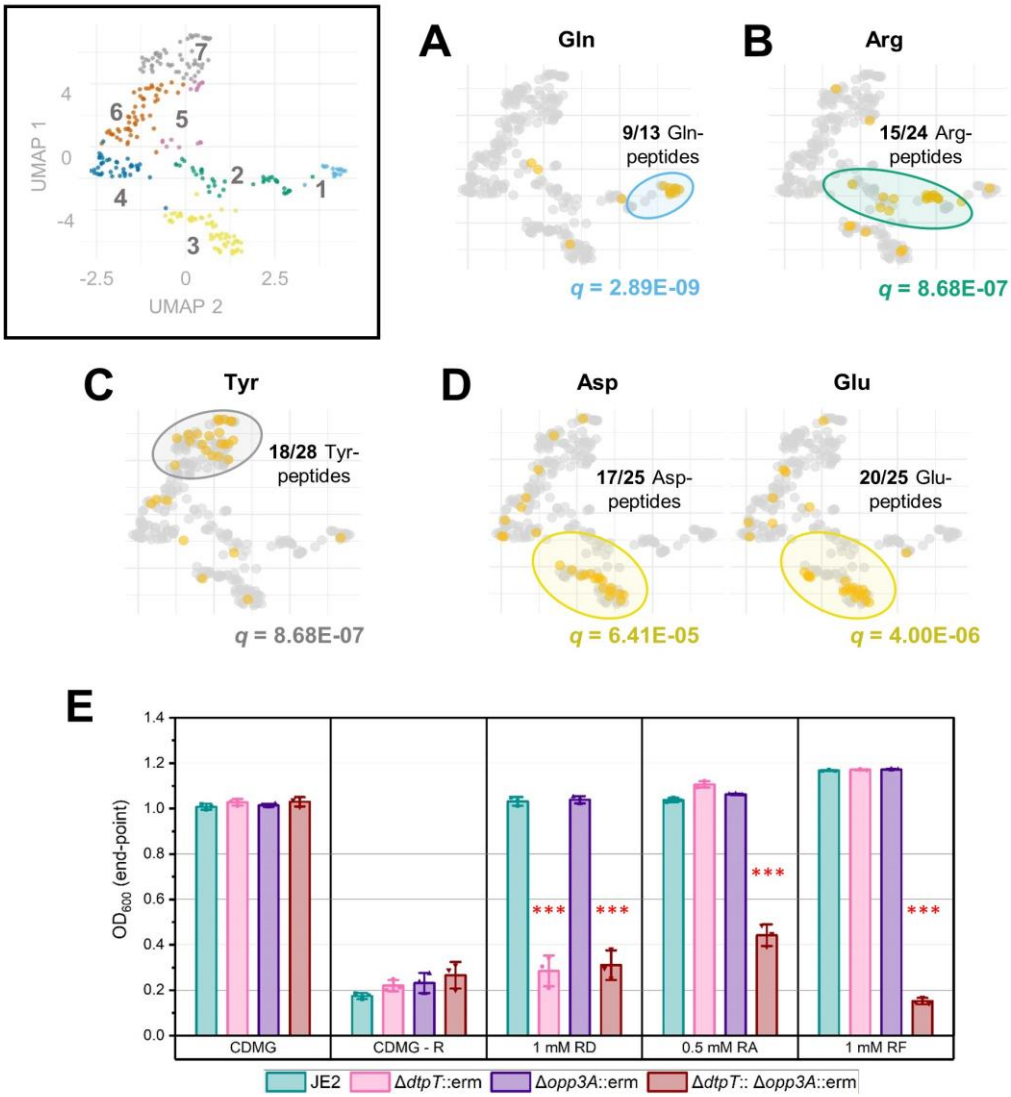

Figure 3 – Specific amino acids are enriched in peptides belonging to a common utilisation pattern. (**A - D**) Enriched amino acids within each cluster were identified via a Fisher exact test with FDR q-value correction. Plots show the position of peptides containing strongly enriched amino acids ($q \leq$ 1E-03) overlayed on the original UMAP plot (as labelled). The value of q is given in each case. (**E**) Growth of *S. aureus* strain JE2 and mutant derivatives in CDMG – R supplemented with three dipeptides, as labelled. Arg-Asp (RD) and Arg-Phe (RF) are each cluster 3 peptides, while Arg-Ala (RA) belongs to cluster 2. Bars show the mean end-point OD_{600} value after 24 hours of growth ± standard deviation. End-point OD is reflective of the maximal cell density observed over this period. *** $p < 0.001$; unpaired t-test.

225

226 **DtpT transports peptides with diverse chemical properties**

227 Peptide utilisation (as determined from phenotype microarrays) produces a composite
228 phenotype representing the combined consequences of peptide internalisation and
229 catabolism, both of which are required to drive cellular metabolism and produce a positive
230 signal. As a result, peptides with limited uptake may produce a positive PM signal if efficiently
231 catabolised while other peptides may be rapidly internalised (by DtpT or otherwise) without
232 producing a positive PM signal due to incomplete catabolic pathways.

233 To measure transport of peptides directly, we expressed and purified *S. aureus* DtpT
234 recombinantly from *E. coli* cells (Figure S2) and reconstituted the pure protein into liposomes
235 (Figure S3A-B), using methods previously applied to study the *Staphylococcus hominis* DtpT
236 orthologue $PepT_{Sh}$ (Minhas et al., 2018). Transport of di/tri-peptide substrates was then
237 assessed by utilising the pH-sensitive dye pyranine, as described previously (Parker et al.,
238 2014). Briefly, peptide transport was assayed by monitoring the acidification of the liposome
239 lumen and quantified over time for each peptide after induction of a negative-inside
240 membrane potential ($\Delta\Psi$) (Figure 4A). To validate this methodology, we confirmed that
241 peptide transport is dependent on the presence of both a valid substrate and $\Delta\Psi$, as
242 evidenced by the lack of strong acidification when either of these components is absent
243 (Figure S3C) and were then able to measure transport for a range of selected di- and
244 tripeptides (Figure 3B-C).

245 By assessing transport of 20 peptides with diverse chemical properties, we were able to
246 confirm DtpT-mediated transport for 12 of the putative substrates identified by our phenotype
247 microarrays, including all Asp-/Glu-containing peptides tested (Figure 4C). We also
248 confirmed the transport of Arg-Phe, Arg-Ala and Arg-Asp by DtpT, as already demonstrated
249 in our Arg-auxotrophy experiments. Overall, there is good agreement between our liposome-
250 based transport assays and whole-cell peptide utilisation methods (Figure 4C). We do note
251 that a small number of peptides are transported by DtpT which did not sustain metabolism
252 of *S. aureus* in the phenotype microarray assay, namely; Ala-Ala, Ala-Ala-Ala and Cys-Gly.
253 Such an observation suggests that peptide internalisation is not the limiting factor in
254 utilisation of these peptides. Additionally, our transport assays shed new light on the
255 molecular factors contributing toward substrate preference in this transporter. For instance,
256 our data demonstrate how many favourable DtpT substrates incorporate acidic amino acids
257 (Arg-Asp and Gly-Glu) or amino acids with small, uncharged side chains (Ala-Ala, Gly-Gly

258 and Gly-Pro) (Figure 4C). In contrast, we demonstrate that dipeptides containing aromatic
259 residues in position 2 generally demonstrate poorer transport when compared to those with
260 less bulky side-chains in the equivalent position. Poor internalisation of these substrates (e.g.
261 Val-Tyr and Ala-Phe) by DtpT is consistent with their lack of utilisation in PM assays (Figure
262 4C). Overall, our transport assays demonstrate that DtpT is highly promiscuous and capable
263 of transporting substrates with a range of chemical structures and properties, which is
264 similarly noted for other POT transporters studied previously (Kotov et al., 2023; Parker et al.,
265 2014).

266

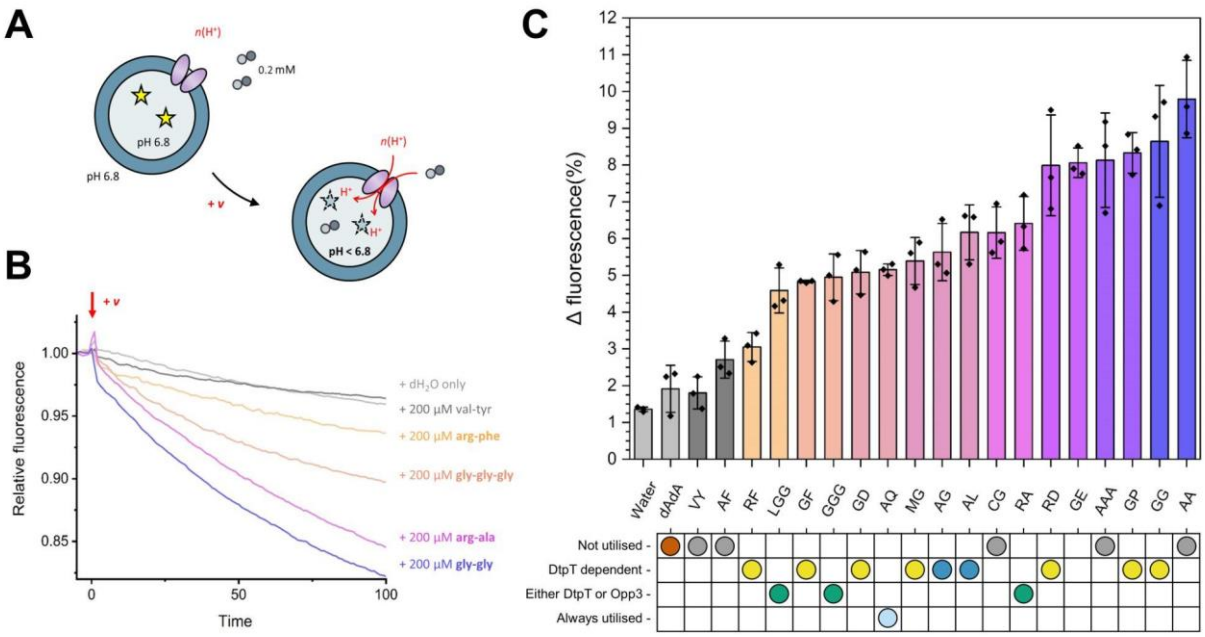

Figure 4 – DtpT transports structurally diverse di/tri-peptides. (**A**) DtpT was reconstituted into liposomes containing pyranine. Upon induction of negative-inside ΔΨ, DtpT transports peptides from the external environment into the liposome lumen. Peptide transport is proton-coupled, leading to acidification of the lumen and a decrease in the pyranine fluorescence (ex. 460 / emm.510). (**B**) Exemplary transport data for 5 peptides normalised immediately before the addition of valinomycin (red arrow) for ease of comparison. Curves show the mean of three replicates. (**C**) Transport of 20 peptides was compared by quantifying the change in pyranine fluorescence over the first 30 seconds of the assay. Bars indicate the mean ± standard deviation. Coloured bars indicate a change in fluorescence which differs significantly from the no peptide ("Water") control, as determined by a one-way ANOVA with Fisher LSD test ($p \leq 0.05$). Peptides are labelled according to their single-letter amino acid code (dAdA = d-ala-d-ala). Corresponding phenotypic patterns identified by PM analysis for each peptide are shown below.

DtpT is a functional glutathione permease

Our phenotype microarray data points toward a distinct role for DtpT in the utilisation of Asp/Glu-containing peptides (Figure 3D), and we have demonstrated that dipeptides in this category are generally favourable transport targets (Figure 4C). Reduced glutathione (GSH) is a biologically important tripeptide metabolite with diverse roles in many organisms, primarily serving as an antioxidant in eukaryotes and some prokaryotes (Lushchak, 2012). GSH consists of a Cys-Gly dipeptide conjugated to glutamate via a γ-linked peptide bond between the glutamate side chain and amino terminus of the cysteine (Figure 5A). Given that DtpT recognises and transports Cys-Gly (Figure 4C), we predicted that DtpT may also transport GSH and that this activity may be relevant in biological environments where glutathione is enriched. To test this, we measured DtpT transport activity with either GSH or oxidised glutathione (GSSG) (Figure 5B). We demonstrate that GSH is transported by DtpT, with the acidification of the liposome lumen over the first 30 seconds comparable to that observed for Cys-Gly. We do not observe the transport of GSSG in this assay, likely due to the larger structure of GSSG compared to GSH.

The Gis system is an ABC-type importer which has recently been characterised as a route of glutathione acquisition in *S. aureus* and is the only known route of uptake for both GSH and GSSG identified in this bacterium to date (Lensmire et al., 2023). However, under conditions where GSH utilisation is essential, the growth of a *gis*-deficient mutant strain is restored to near wild-type levels when GSH is supplied at concentrations greater than 0.5 mM (Lensmire et al., 2023). This implies the existence of at least one additional route of GSH uptake. To determine whether DtpT fulfils this role, isogenic mutants of *dtpT* and *gisD,* as well as a double mutant, were grown under conditions where glutathione was supplied as the sole sulphur source. At 50 μM GSH, we found that the growth of *S. aureus* is limited and solely dependent on the Gis system (Figure S4A). However, both single mutant strains demonstrated growth defects relative to the wild-type at 1 mM GSH, while growth was abolished for the double mutant under this condition (Figure 5C). In comparison, we found that growth in the presence of GSSG was solely dependent on Gis (Figure S4B). We also found that *in trans* complementation with *dtpT* was sufficient to fully restore growth of the *dtpT* single-mutant and partially restore growth in the double mutant strain in the presence of 1 mM GSH (Figure 5D). Finally, given that GSH oxidises spontaneously over time in aerated environments, we repeated the growth experiment with 1 mM GSH under anaerobic conditions to limit changes in the oxidation state of GSH during growth (Figure S4C). Again, we observed phenotypes which were consistent with those observed during aerobic growth.

303 Taken together, these observations demonstrate that both Gis and DtpT contribute to GSH
304 uptake at millimolar concentrations.

305

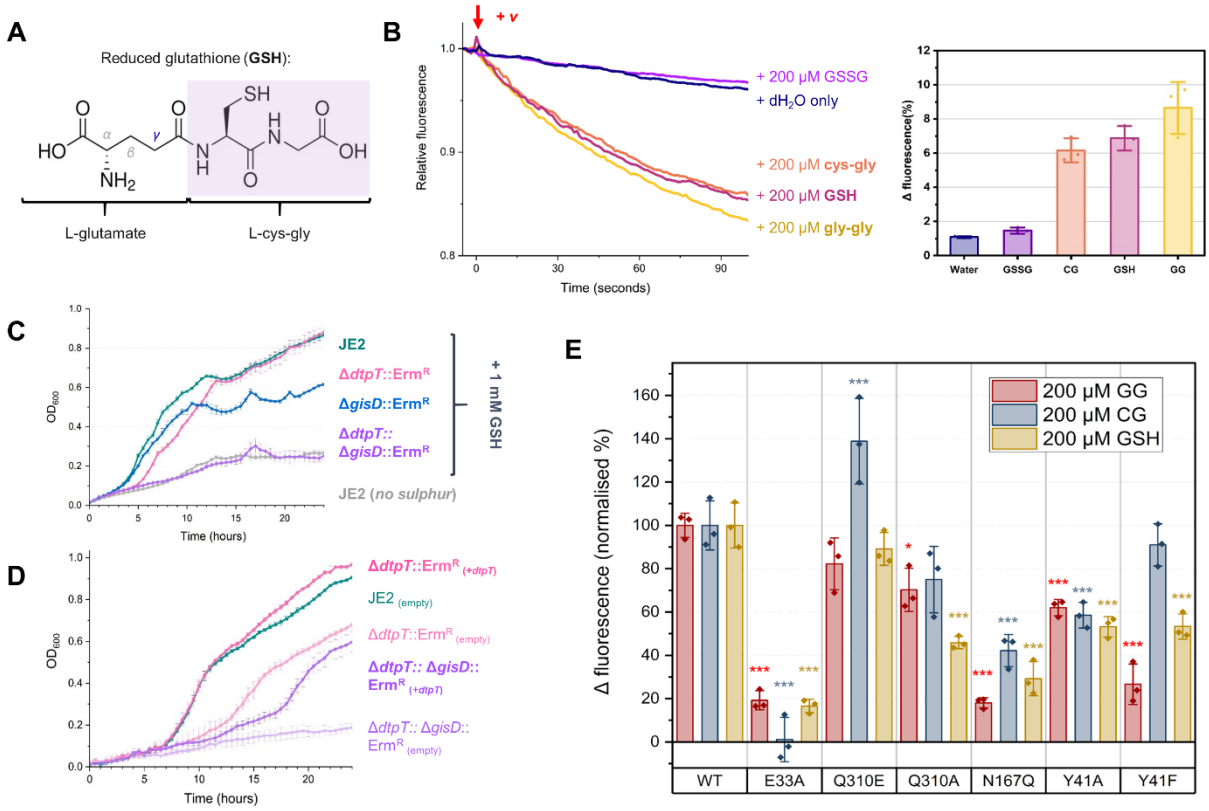

Figure 5 – DtpT transports reduced glutathione (GSH). (**A**) Chemical structure of GSH. (**B**) (**Left**) Transport of GSH and GSSG was assessed via pyranine transport assays. Transport assay curves are normalised immediately before the addition of valinomycin (red arrow) for ease of comparison. Curves show the mean of three replicates. (**Right**) summarised transport data. Bars show the mean of three replicates ± standard deviation. (**C - D**) Growth of *S. aureus* strain JE2 and mutant derivatives was assessed in CDMG – *s* supplemented with 1 mM GSH. In each case, strains were grown over 24 hours and OD_{600} was measured every 30 minutes for three biological replicates. Curves indicate the mean values ± standard deviation. (**C**) Growth of single-mutants of *dtpT* and *gisD* as well as a *dtpT gisD* double-mutant strain in CDMG – *s* ± 1 mM GSH. (**D**) *In-trans* expression of DtpT restores growth of the *dtpT* single mutant to wild-type levels and partially restores growth in the *dtpT gisD* double mutant. (**E**) Transport data for DtpT mutant variants against Gly-Gly, Cys-Gly and GSH, expressed as a percentage of the activity for the wild-type protein. Bars indicate the mean ± standard deviation. *p<0.05, **p<0.01, ***p<0.001; One-way ANOVA with Tukey's test.

306

307 In order to better understand the structural determinants underpinning GSH transport in
308 DtpT, mutant variants were generated with alterations in residues predicted to be involved in
309 substrate binding and transport (Figure 5E, Figure S5-6). Glu33 and Tyr41 form part of the
310 conserved E_{33}xxERFxYY_{41} motif found ubiquitously in POT transporters and are known to
311 contribute toward proton coupling during the transport cycle (Aduri et al., 2015; Lichtinger et
312 al., 2024; Solcan et al., 2012) (Figure S5). Consistent with this, acidification of the liposome
313 lumen was severely reduced in an E33A mutant to levels equivalent to that observed for wild-
314 type DtpT in the absence of substrate (Figure S6), demonstrating that Glu33 is essential for
315 proton-coupled transport in this protein. Acidification was similarly reduced for all substrates
316 in the Y41A mutant protein, though to a lesser extent (Figure 5E). Similarly, Asn167 is
317 conserved across diverse POT proteins and has been observed to facilitate substrate binding
318 via anchoring of the peptide N-terminal amide group (Kotov et al., 2023; Lyons et al., 2014)
319 (Figure S5). As expected, the transport of gly-gly and cys-gly is restricted in an N167Q mutant
320 likely due to substrate occlusion. Transport of GSH is also restricted in this mutant, providing
321 evidence that Asn167 plays a key role in transporting this novel substrate.

322 Based on co-crystal structures of the *Streptococcus thermophilus* POT protein $PepT_{St}$ solved
323 in complex with Ala-Phe and Ala-Ala-Ala, a dual-binding model has been proposed in which
324 POTs differentially accommodate dipeptides and tripeptides during transport (Lyons et al.,
325 2014). Briefly, these structures suggest that dipeptides bind in a lateral conformation (relative
326 to the membrane plane), while tripeptides can be accommodated in an alternative vertical
327 conformation in which the peptide extends deeper into the binding groove and interacts with
328 residues adjacent to the extracellular gate. In this conformation, the carboxyl terminus of Ala-
329 Ala-Ala is coordinated by interactions with Glu299 and Glu300. Gln310 in the *Staphylococcus*
330 *hominis* POT $PepT_{Sh}$ (conserved in the *S. aureus* DtpT studied here, Figure S5) is orthologous
331 to Glu299 and was similarly found to form part of a deep pocket involved in accommodating
332 the thioalcohol moiety of a vertically bound S-Cys-Gly-3M3SH ligand (Minhas et al., 2018).
333 Here, we observe that the transport of GSH is significantly reduced in a Q310A variant of
334 DtpT (Figure 5E). Such an observation, therefore, implicates Gln310 in the coordination of
335 GSH, suggesting that GSH may be accommodated in a similar position to S-Cys-Gly-3M3SH
336 in $PepT_{Sh}$, and may indicate a unique mechanism for recognising sulphur-containing
337 peptides.

338

339 **Glutathione transport-deficient strains demonstrate reduced fitness during**
340 **macrophage infection**

341 Although *S. aureus* was historically considered an extracellular pathogen, recent work has
342 demonstrated that this bacterium survives inside phagocytic cells, highlighting how its
343 intracellular lifestyle may contribute to dissemination and immune evasion during systemic
344 infection (Flannagan et al., 2016; Kubica et al., 2008). To date, there is a poor understanding
345 of the molecular factors governing fitness in these intracellular environments, particularly
346 regarding nutrient availability and acquisition. Cytosolic concentrations of GSH in human
347 cells range from 1 to 10 mM depending on the cell type, making it the most abundant
348 intracellular non-protein thiol (Cui et al., 2023; Meister, 1988). Based on this, we hypothesised
349 that glutathione utilisation may contribute toward the fitness of *S. aureus* in intracellular
350 environments.

351 Differentiated THP1 macrophage-like cells and human monocyte-derived macrophages
352 (hMDMs) were each infected with either JE2 or mutant derivatives of *dtpT* and/or *gisD*, and
353 bacterial survival was quantified over the first 8 hours post-infection (Figure 6). To account
354 for any changes in fitness resulting from the inclusion of the *bursa aurealis* transposon
355 insertion sequence, we also assessed the survival of a mutant strain carrying the transposon
356 in a presumed phenotypically-null locus corresponding to a predicted IS3-family transposase
357 gene (SAUSA300_0060). In THP-1 cells, survival of both the *dtpT* and *gisD* single-mutant
358 strains was reduced slightly on-average at 8 hours but did not differ significantly when
359 compared to the wild-type. In comparison, survival of the *dtpT gisD* double mutant strain was
360 significantly lower at this time-point, being reduced more than two-fold relative to the wild-
361 type (Figure 6A). Similarly, survival of both the *gisD* single-mutant and *dtpT gisD* double-
362 mutant strains was significantly reduced at this time-point in hMDMs derived from eight
363 independent donors (Figure 6B). Overall, these data suggest that GSH transport is required
364 for complete fitness of *S. aureus* during macrophage infection, though the presence of either
365 *dtpT* or *gisD* is seemingly sufficient to restore survival to near wild-type levels.

366 In eukaryotic systems, glutathione acts as an important cellular antioxidant and contributes
367 to varied physiological processes including metal homeostasis and alleviation of lipid
368 oxidation stress, ultimately contributing to immune cell function (Dasgupta et al., 2010;
369 Lushchak, 2012). We, therefore, wondered whether bacterial sequestration of glutathione
370 may serve as a strategy to disrupt healthy phagocyte function and thereby promote bacterial

371 survival. On average, we found no differences in cytotoxicity between the tested strains at 4
372 hours post-infection (Figure S7B). In contrast, we observed that THP1 cells infected with the
373 GSH transporter-null double-mutant strain demonstrated increased cell death at 8 hours
374 relative to the wild-type (Figure S7B). To investigate this further, we quantified the production
375 of inflammatory cytokines at 6 hours post-infection, representing the mid-point between
376 these two states. At this time point, cells infected with the double-mutant strain produced
377 significantly lower levels of both IL-1β and IL6, though production of TNFα was seemingly
378 unaffected (Figure S7C). While preliminary, these observations suggest that glutathione
379 transporters allow *S. aureus* to modulate the macrophage pro-inflammatory status and
380 maintain the intracellular niche by ultimately prolonging host-cell survival.

381

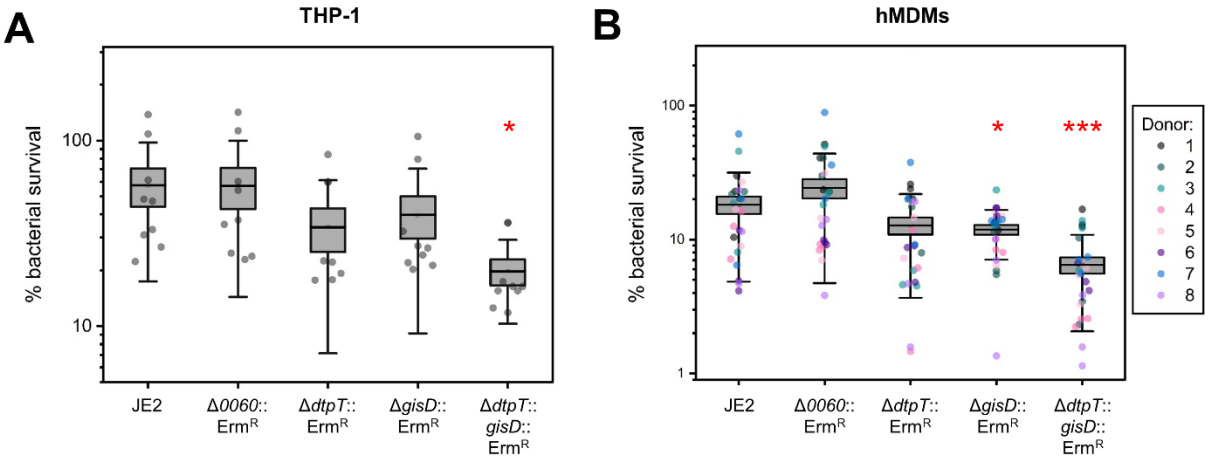

Figure 6. A glutathione transport-null double-mutant demonstrates reduced survival inside macrophages. (**A - B**) Bacterial survival of JE2 and mutant derivatives after 8 hours post-infection in THP1 macrophage-like cells (**A**; *n* = 9) and hMDM cells (**B**; *n* = 8 donors, each infected in biological triplicate). In each case, survival is calculated as a percentage of the total bacterial uptake, as determined at 30 minutes post-infection. In each case *p<0.05, **p<0.01, ***p<0.001; as determined by paired-sample t-test.

382

383 ## Discussion
384

385 The promiscuous nature of peptide transport proteins and their functional redundancy in
386 many organisms have made these systems historically challenging to characterise regarding
387 substrate range and preference. Molecular dynamics simulations and similar computational
388 methods have been combined with biochemical and structural methods in order predict
389 substrate preferences in POTs, but experimental evidence for the applicability of these
390 models to biological systems is lacking (Kotov et al., 2023; Li et al., 2022; Samsudin et al.,
391 2016). Here, we present an extensive cell-based analysis of peptide transporter function in
392 *S. aureus* and apply biochemical analysis of DtpT to both verify and expand our functional
393 understanding of this transporter. Our findings demonstrate that DtpT is highly promiscuous,
394 evidenced by the considerable heterogeneity observed among putative transport targets
395 identified here. While earlier work has focussed on the contribution of Opp3 toward the
396 utilisation of host-derived peptides (Lehman et al., 2019), our data instead highlights how
397 DtpT serves as a major route of uptake for diverse dipeptides and tripeptides in *S. aureus*,
398 including GSH. Indeed, this broad substrate range may underpin the essentiality of DtpT
399 previously observed in various systemic animal infection models (Coulter et al., 1998).

400 A number of recent studies have demonstrated how exogenous amino acids play diverse
401 functional roles during *S. aureus* infections, serving both as key nutrient sources and
402 environmental signals with defined regulatory consequences (Urso et al., 2024). Despite this,
403 many studies overlook the potential contribution of host-derived oligopeptides as reservoirs
404 for these amino acids. For instance, glutamate is known to serve as a major gluconeogenic
405 carbon source for *S. aureus* and strains lacking the glutamate dehydrogenase GudB are
406 attenuated under glucose-limited conditions (Halsey et al., 2017). Glutamate restriction has
407 pleiotropic effects on cellular physiology, ultimately resulting in increased biofilm formation
408 *in vitro* and *in vivo* (Shibamura-Fujiogi et al., 2022). Taken together, these observations
409 implicate exogenous glutamate as an important factor contributing to both growth and
410 environmental sensing in *S. aureus*. Acquisition of exogenous glutamate in *S. aureus* is
411 primarily facilitated by the amino acid permease GltS (Zeden et al., 2020). Here, we
412 demonstrate that DtpT is responsible for the utilisation of diverse glutamate-containing
413 dipeptides and show that these peptides are specifically enriched among DtpT substrates
414 (Figure 3A). These findings suggest that DtpT-mediated peptide uptake may serve as an
415 additional source of exogenous glutamate in peptide-rich growth environments.

416 Our PM data reinforces the fact that DtpT serves as the primary route of dipeptide uptake in
417 *S. aureus*, but also reveals some overlap in substrate specificity between this transporter and
418 Opp3. The identification of a subset of peptides with redundant routes of internalisation may
419 point toward these peptides being of high value to the cell, perhaps serving as reservoirs for
420 important amino acids in relevant biological contexts. For instance, our data demonstrates
421 how diverse arginine-containing dipeptides are utilised by *S. aureus*, being significantly
422 enriched within the cluster of peptides utilised via either DtpT or Opp3 in our PM data (Figure
423 2; 3B). Consistent with this, *S. aureus* USA300 rapidly internalises arginine during growth but
424 converts neither proline nor glutamate to arginine when grown *in vitro*, making exogenous
425 arginine essential for growth (Halsey et al., 2017; Reslane et al., 2022). Experimental evidence
426 has demonstrated how arginine restriction stimulates antibiotic tolerance in *S. aureus*
427 biofilms, implicating arginine availability as an important environmental stimulus modulating
428 *S. aureus* cell behaviour (Freiberg et al., 2024). We propose that the redundancy observed
429 here for uptake of Arg-containing peptides likely signifies an evolutionary strategy to increase
430 the diversity of potential arginine sources available to the cell, which is in agreement with the
431 apparent importance of exogenous arginine in *S. aureus* physiology. Furthermore, the
432 presence of two Arg-peptide transporters with varying substrate affinities in *S. aureus* may
433 facilitate the utilisation of these peptides in varied growth environments with variable Arg-
434 containing peptide availability.

435 In a similar vein, DtpT is capable of transporting the glutamine-containing dipeptide Ala-Gln
436 (Figure 4C), but our PM data points toward the existence of a yet-unidentified additional
437 utilisation system which is specific for glutamine-containing peptides (Figure 3A). The
438 existence of such a system may indicate a yet underappreciated role for exogenous
439 glutamine in *S. aureus* physiology. The Opp4 transport system is a yet-uncharacterised Opp-
440 homologue which is widespread in *S. aureus* and is likely to have been generated via
441 duplication of Opp3 (Yu et al., 2014). Given their close evolutionary relationship, we propose
442 that Opp4 is likely to be a peptide transporter like Opp3 and is, therefore, a strong candidate
443 to fulfil the role of the alternative Gln-peptide transport system in *S. aureus*. While ACME Opp
444 may also contribute toward peptide transport, this system is more closely related to Opp1/2
445 and is, therefore, more likely to play a role in metal ion transport.

446 In contrast to the examples listed above, we demonstrate that tyrosine-containing dipeptides
447 are scarcely utilised by *S. aureus* (Figure 3C). This is perhaps unsurprising, given that *S.*
448 *aureus* JE2 lacks a complete catabolic pathway for tyrosine utilisation and does not rapidly

449 consume exogenous tyrosine when grown in defined media (Halsey et al., 2017). Intriguingly,
450 no DtpT-mediated transport was observed for the sole tyrosine-containing peptide (Val-Tyr)
451 assessed here (Figure 4B-C), providing evidence that DtpT possesses a distinct biochemical
452 preference toward peptides which are readily catabolised over those which lack the potential
453 to serve as a nutrient source. That being said, we do observe the utilisation of some
454 dipeptides exclusively composed of the branched-chain amino acids (i.e. leucine, isoleucine
455 and valine) and demonstrate that several such peptides are utilised via DtpT, despite the lack
456 of a known catabolic pathway for these amino acids in JE2 (Halsey et al., 2017). For instance,
457 we demonstrate that Leu-Leu is utilised robustly by JE2 and belongs to cluster 2, implicating
458 both DtpT and Opp3 in the transport of this peptide (Figure 2). Our findings, therefore,
459 suggest that branched chain amino acids derived from short peptides are catabolised by
460 JE2, though the catabolic pathways involved remain to be elucidated.

461 Glutathione is a ubiquitous metabolite in eukaryotic systems and is the predominant thiol
462 present in intracellular niches, as well as being enriched in other environments associated
463 with *S. aureus* infection including the sputum of cystic fibrosis patients (Shull et al., 2024). In
464 most biological contexts, GSH is the most abundant form of glutathione by a significant
465 margin (Hansen et al., 2009). Here, we identify GSH as a substrate of DtpT and demonstrate
466 that either DtpT or Gis-mediated transport is sufficient to meet the nutrient sulphur
467 requirements of *S. aureus* at physiologically relevant GSH concentrations (Figure 5C). To the
468 best of our knowledge, our findings provide the first example of a bacterial POT contributing
469 toward glutathione acquisition; whether or not this function is conserved in the wider POT
470 superfamily remains unclear, especially given that Gln310 (or Glu in the equivalent position)
471 is required for strong transport of GSH but this feature is not conserved across bacterial POT
472 proteins (Figure 5E; Figure S5).

473 Generally, binding-protein dependant transport systems (including ABC transporters)
474 operate with high affinities, whilst POTs and similar MFS systems have been reported as
475 having substrate affinities in the high-micromolar or low millimolar range (Kotov et al., 2023;
476 Samsudin et al., 2016). We, therefore, predict that Gis may serve as the dominant system
477 involved in GSH scavenging under conditions where the metabolite is scarce, whilst both
478 systems likely contribute to transport in GSH-enriched environments. Indeed, the
479 phenotypes associated with our mutant strains support such a model (Figure 5C; Figure S4).

480 Finally, we identify *S. aureus* glutathione transporters as important fitness determinants
481 during intracellular growth inside macrophages, representing an environment in which GSH
482 is present at millimolar concentrations (Figure 5A-B). In *Mycobacterium tuberculosis* (Mtb),
483 glutathione transport has been implicated in regulating the activity of Mtb-infected
484 macrophages and thereby contributing toward intracellular survival and immune evasion
485 (Dasgupta et al., 2010). Our macrophage infection data similarly demonstrates how the
486 presence of glutathione transporters affects host-cell behaviour, seemingly allowing the
487 pathogen to modulate innate immune signalling responses and subvert premature host-cell
488 death (Figure S7). Hence, glutathione transport may represent a conserved strategy utilised
489 by intracellular bacterial pathogens in order to enable long-term intracellular survival, thereby
490 avoiding exposure to extracellular stresses and immune clearance. More work is needed to
491 better understand how the host-cell response is modified as a result of bacterial glutathione
492 transport and determine whether this response is conserved across different host-cell types.

493 Overall, this work has significantly expanded our knowledge of peptide utilisation in *S. aureus*
494 and shed light on a novel role for glutathione transport in host-pathogen interactions during
495 intracellular infection. However, with the diversity of roles ascribed to peptide transporters in
496 other organisms – including cell-wall turnover (Maqbool et al., 2011; Park et al., 1998;
497 Simpson et al., 2023), antimicrobial peptide resistance (Parra-Lopez et al., 1993; Rivera et
498 al., 2024) and cell signalling (Dubois et al., 2019; Nasher et al., 2018; Zheng et al., 2018) – it
499 is clear that this is an area of *S. aureus* biology where much remains to be discovered and
500 understood.

501

502 # Methods
503

504 ## Bacterial strains and growth conditions

505 All *S. aureus* strains used in this study were routinely cultured in tryptic soy broth (TSB) with
506 shaking or on solid tryptic soy agar (TSA) medium at 37°C. *E. coli* strains were routinely
507 cultured in lysogeny broth (LB) with shaking or on LB agar at 37°C. Selective antibiotics were
508 added during growth when appropriate at the following concentrations: 50 µg/ml kanamycin,
509 100 µg/ml ampicillin, 10 µg/ml erythromycin, 10 µg/ml chloramphenicol.

510 *S. aureus* JE2 transposon mutants were acquired from the Nebraska Transposon Mutant
511 Library (NTML; (Fey et al., 2013) and transduced into wild-type JE2 via Φ85 bacteriophage in
512 order minimise off-target genetic inconsistencies between strains. To generate double
513 mutant strains, the Erm^R resistance cassette was exchanged with an unmarked sequence
514 using the allelic exchange vector pTnT, as described previously (Bose et al., 2013). Plasmids
515 were generated using the ClonExpress II One Step Cloning Kit (Vazyme) according to
516 manufacturer's instructions. DtpT complementation in *S. aureus* mutant strains was achieved
517 via introduction of the entire *dtpT* locus into the *E. coli* / *S. aureus* shuttle vector pSK5630
518 modified by the addition of the native *dtpT* promoter sequence (herein referred to as $pSK56_{pT}$)
519 (Grkovic et al., 2003).

520 A full list of bacterial strains utilised in this work are provided in supplemental table ST1.
521 Primers utilised for diagnostic PCR, cloning and sequencing of genetic elements are provided
522 in supplemental table ST2.

523 ## Phenotype microarrays and analysis

524 Peptide utilisation by *S. aureus* strain JE2 and mutant derivatives was assessed on
525 phenotype microarray plates PM 6-8 (Biolog) using a modified version of the manufacturer's
526 protocol. Cells grown on TSA overnight were transferred from solid media into 3 ml IF-0α
527 buffer using a sterile cotton swab and pelleted. Cells were washed twice and resuspended
528 in IF-0α. This cell suspension was then diluted to a final OD_{600} of 0.004 in 9.975 ml IF-0α and
529 supplemented with 110 µl redox dye H (Biolog) and 915 µl 12X PM additive solution (240 mM
530 tricarballylic acid, pH 7.1; 24 mM $MgCl_2$; 12 mM $CaCl_2$; 150 µM L-cystine, pH 8.5; 0.06% w/v
531 yeast extract; 0.06% v/v tween 80; 6 mM D-glucose; 12 mM pyruvate). PM plates were
532 inoculated with 100 µl/well of the prepared cell suspension and incubated for 36 hours at

533 37°C with continuous slow shaking in an Epoch2 microplate spectrophotometer (Agilent).
534 OD_{590} and OD_{750} were measured every 15 minutes.

535 Signal curves (OD_{590} - OD_{750} against time) for all four strains were grouped for each peptide
536 and then analysed by Uniform Manifold Approximation and Projection (UMAP) using the
537 UMAP R library and a random seed of 888 (McInnes et al., 2018). K-means clustering was
538 used on the same grouped data with "kmeans" R function and k=7. Empirical area under the
539 curve (eAUC) was calculated using Growthcurver (Sprouffske & Wagner, 2016).

540 **Peptide utilisation assays**

541 Utilisation of specific peptides was assessed using glucose-supplemented chemically
542 defined medium (CDMG) based on a previously reported methodology (Hussain et al., 1991).
543 The complete composition of the CDMG used here is provided in supplemental table ST3.
544 For assessing the utilisation of arginine-containing peptides, L-arginine was omitted from the
545 medium (CDMG - *R*). For assessing the utilisation of glutathione, L-cysteine and L-methionine
546 were omitted from the medium and $(NH_4)_2SO_4 \cdot FeSO_4 \cdot 6H_2O$ was substituted for 15 µM iron
547 (III) citrate (CDMG - *s*). Reduced glutathione solutions were prepared under anaerobic
548 conditions to prevent changes in the oxidation state before commencing assays. Overnight
549 cultures of *S. aureus* strain JE2 and mutant derivatives were diluted 1:100 into fresh TSB and
550 grown to mid-exponential phase. Cells were then pelleted and washed twice in the assay
551 medium (CDMG - *R* or CDMG - *s*) before being resuspended and diluted to a final OD_{600} of
552 0.05 in peptide-supplemented medium. 200 µl of each cell suspension was transferred to a
553 Costar 96 well plate (Corning) and incubated for 24 hours at 37°C with shaking. OD_{600} was
554 measured every 30 minutes.

555 For anaerobic growth assays, cultures were prepared as before being transferred to a Whitley
556 A85 anaerobic workstation (Don Whitley Scientific) and diluted into assay medium which had
557 been equilibrated under anaerobic conditions for at least 3 hours and supplemented with 100
558 mM sodium nitrate. Growth was monitored as above in a Stratus 96 well plate reader (Cerillo)
559 for 18 hours at 37°C without shaking.

560 **Protein purification**

561 The DtpT open reading frame was amplified directly from the *S. aureus* JE2 genome and
562 cloned into the C-terminal octa-histidine/GFP-tagged fusion vector pWaldo (Drew et al.,
563 2006) before being transformed into *E. coli* C43(DE3) (Miroux & Walker, 1996). Mutant

564 variants were generated via site-directed PCR mutagenesis and blunt-end ligation with T4
565 DNA ligase (NEB) and all constructs were verified by sequencing.

566 Cells grown overnight in LB supplemented with kanamycin were diluted 1:100 into fresh
567 media. Cultures were incubated at 37°C until an OD_{600} of 0.5 was reached. Expression was
568 then induced by the addition of IPTG to a final concentration of 100 μM. Cultures were
569 incubated overnight at 25°C with shaking. Cells were then pelleted, resuspended in 50 ml
570 resuspension buffer (40 mM Tris, pH 7.5; 10% glycerol) and lysed by sonication. Crude
571 lysates were clarified via centrifugation at 27,000 x g for 30 minutes. Membranes were then
572 pelleted via ultracentrifugation at 164000 x g for 120 minutes. Membrane pellets were pooled
573 and resuspended in 40 ml protein solubilisation buffer (40 mM Tris, pH 7.5; 200 mM NaCl; 20
574 mM imidazole; 10% glycerol; 0.5% n-dodecyl-B-pyromaltoside (DDM)) using a glass
575 homogenizer before being incubated for 60 minutes at 4°C with rolling. The resultant
576 suspension was then ultracentrifuged as before for 60 minutes to pellet leftover membranes
577 and insoluble contaminants. Supernatant containing the solubilised membrane proteins was
578 pooled and applied to a His-TRAP nickel affinity column (GE Healthcare) using an ÄKTA
579 Protein Purification System (Cytiva). This column was washed with 50 ml column wash buffer
580 (40 mM Tris, pH 7.5; 200 mM NaCl; 20 mM imidazole; 10% glycerol; 0.04% DDM) and the
581 fusion protein was then eluted via application of column elution buffer (40 mM Tris, pH 7.5;
582 200 mM NaCl; 400 mM imidazole; 10% glycerol; 0.04% DDM).

583 Purified protein was exchanged into TEV reaction buffer (40 mM Tris, pH 7.5; 200 mM NaCl;
584 0.5 mM EDTA; 1 mM DTT; 10% glycerol; 0.04% DDM) using a HiTRAP desalting column
585 (SLS). Protein was then mixed with TEV protease to a final ratio of approximately 3:1. The
586 resultant reaction mixture was incubated overnight at 4°C. Pure DtpT was isolated by
587 applying the reaction mixture to a His-TRAP nickel affinity column as before and washing
588 with column wash buffer, this time collecting the flow-through fractions. Pure protein was
589 stored at -70°C.

590 **Reconstitution into proteoliposomes and transport assays**

591 Purified DtpT was exchanged into reconstitution buffer (20 mM Tris pH 7.5; 150 mM NaCl;
592 0.03% DDM) and diluted to a final concentration of 0.5 mg/ml. Liposomes (composed of
593 POPE and POPG in a 3:1 ratio) were prepared and extruded 11 times each through pre-
594 soaked 0.8 μm and 0.4 μm track-etched polycarbonate membranes (Whatman) before
595 diluting to a final concentration of 10 mg/ml in liposome buffer (50 mM KPi, pH 7).

596 10 mg lipid mixture was gradually added to 200 µg protein at room temperature before being
597 incubated on ice for 60 minutes. 100 µl SM2 Biobeads (Biorad) suspended in water were
598 added to the lipid-protein mixture, which was then incubated for 1 hour at 4°C while rotating.
599 A further 130 µl Biobeads were added and the mixture was incubated as before for a further
600 3 hours. Biobeads were pelleted and the lipid-protein mixture was transferred to a fresh tube.
601 160 µl Biobeads were added and the mixture was incubated as before for a further 16 hours.
602 Biobeads were removed as before and proteoliposomes were pelleted via ultracentrifugation
603 at 158 000 × g for 30 minutes. Proteoliposomes were then resuspended in liposome buffer
604 to a final protein concentration of 0.5 mg/ml (assuming 100% reconstitution efficiency) and
605 subjected to three freeze-thaw cycles before dialysing extensively against liposome buffer at
606 4°C. Proteoliposomes were pelleted as before and resuspended in liposome buffer before
607 being stored at -70°C.

608 For transport assays, proteoliposomes were pelleted as before and resuspended in inside
609 buffer (5 mM HEPES, pH 6.8; 120 mM KCl; 2 mM $MgSO_4$) spiked with 1 mM pyranine.
610 Proteoliposomes were subjected to seven freeze-thaw cycles before being extruded through
611 a pre-soaked 0.4 µm track-etched polycarbonate membrane. Proteoliposomes were then
612 pelleted at 20°C and resuspended in inside buffer. Excess pyranine was removed using a
613 microspin G25 desalting column (Cytiva) according to the manufacturer's protocol.
614 Liposomes were finally pelleted again at 20°C and resuspended to a final protein
615 concentration of 1 mg/ml. For each assay, 6 µg of proteoliposomes were diluted 1:100 into
616 outside buffer (5 mM HEPES, pH 6.8; 120 mM NaCl; 2 mM $MgSO_4$). Assays were performed
617 in 1 ml clear plastic microcuvettes using a Fluoromax-4 spectrophotometer (Horiba) with a
618 magnetic flee for stirring. Fluorescence of pyranine was measured via excitation at 460 nm
619 and emission at 510 nm. Substrate was added to the reaction at t = 25 s and transport was
620 induced by the addition of 1 µM valinomycin at t = 50 s.

621 **Macrophage culture and differentiation**

622 THP1 cells (ATCC) were cultured in macrophages media (RPMI1640 supplemented with 10%
623 Fetal Calf Serum and Glutamine). To obtain a macrophage-like differentiation state, THP1
624 were differentiated for 48 hrs in macrophage media supplemented with 50 ng/mL Phorbol
625 12-myristate 13-acetate (in DMSO, Sigma-Aldrich). PMA-containing media was replaced with
626 fresh macrophage media and cells were rested overnight prior to infection.

627 Human primary macrophages were differentiated from human peripheral blood mononuclear
628 cells (PBMCs) obtained from the NHS (University of York Biology ethic committee project
629 DB202111) and differentiated in complete macrophage media supplemented with 50 ng/mL
630 macrophage colony-stimulating factor (mCSF, Proteintech) over 7 days.

631 **Macrophage infection**

632 Infection of macrophages and macrophage-like cell lines was carried out based on previously
633 published methods (Alves et al., 2024). Overnight cultures of *S. aureus* strain JE2 and mutant
634 derivatives were diluted 1:100 into fresh TSB and grown to mid-exponential phase. Cells
635 were then pelleted and washed twice in ice-cold phosphate-buffered saline (PBS) before
636 being resuspended to a final cell density of 5 x 10^7 CFU/ml. For infection, 10 µl bacterial
637 suspension was added to 50,000 hMDM or THP-1 cells (D.O.I. = 10) in 90 µl Opti-MEM
638 reduced serum media (Thermo Fisher) and plates were centrifuged for 5 minutes at 500 x g
639 to promote contact. After 30 minutes of incubation at 37°C, the medium was exchanged for
640 Opti-MEM supplemented with 100 µg/ml gentamicin. The addition of gentamicin was
641 designated t = 0 h. After a further 30 minutes of incubation this medium was removed and
642 cells were then maintained in Opti-MEM supplemented with 5 µg/ml gentamicin (Gibc).

643 To compare bacterial internalisation and survival, cells at t = 0.5 / 8 h were incubated in
644 deionised water for 10 minutes before being lysed by repeated pipetting. Suspensions were
645 serially diluted in PBS, spotted onto TSA and incubated overnight at 37°C to determine viable
646 CFU. Cytotoxicity was measured by quantifying the activity of lactate dehydrogenase (LDH)
647 in the extracellular medium (Cytotox 96 non-radioactive cytotoxicity kit, Promega) and
648 normalised against cells lysed by 0.04% Triton X-100. Cytokine levels in cell culture medium
649 were determined at t = 6 h by utilising human IL 1-β, IL 6 and TNF-α ELISA assay kits
650 (invitrogen) according to the manufacturer's protocols.

Author contributions

Imran Khan: Conceptualization, Formal analysis, Investigation, Methodology, Data processing, Writing – original draft, review & editing. **Sandy MacDonald**: Formal analysis, Data Processing. **Sigurbjorn Markusson**: Investigation. **Callum Robson:** Investigation. **Joanne L Parker**: Conceptualization, Methodology. **Simon Newstead**: Conceptualization, Methodology. Writing – review & editing. **Dave Boucher**: Conceptualization, Investigation, Methodology, Writing – review & editing. **Marjan Van Der Woude**: Conceptualization, Methodology, Supervision, Project administration, Funding acquisition, Writing – review & editing. **Gavin H Thomas**: Conceptualization, Methodology, Supervision, Project administration, Funding acquisition, Writing – review & editing.

Acknowledgements

We are extremely grateful to the Burgess family for the award of a gift to the University of York that supported a PhD studentship to IK. We thank Dr Rebecca M. Corrigan (ORCiD: 0000-0002-6031-1148) for supplying the wild-type JE2 and NTML strains utilised in this study, and for providing valuable technical guidance. We acknowledge ongoing support of the GHT lab through BB/X003035/1.

669 ## References

670 1. Ackroyd, B. K., Dodson, E. J., Mehboob, J., Dowle, A. A., Thomas, G. H., & Wilkinson, A. J.
671 (2024). Structure and ligand binding in the putative anti-microbial peptide transporter
672 protein, YejA. *Microbiology (Reading, England)*, *170*(2).
673 2. Adolf, L. A., Müller-Jochim, A., Kricks, L., Puls, J.-S., Lopez, D., Grein, F., & Heilbronner, S.
674 (2023). Functional membrane microdomains and the hydroxamate siderophore transporter
675 ATPase FhuC govern Isd-dependent heme acquisition in Staphylococcus aureus. *Elife*, *12*.
676 3. Aduri, N. G., Prabhala, B. K., Ernst, H. A., Jørgensen, F. S., Olsen, L., & Mirza, O. (2015). Salt
677 bridge swapping in the EXXERFXYY motif of proton-coupled oligopeptide transporters. *The*
678 *Journal of Biological Chemistry*, *290*(50), 29931–29940.
679 4. Alves, J., Vrieling, M., Ring, N., Yebra, G., Pickering, A., Prajsnar, T. K., Renshaw, S. A., &
680 Fitzgerald, J. R. (2024). Experimental evolution of Staphylococcus aureus in macrophages:
681 dissection of a conditional adaptive trait promoting intracellular survival. *MBio*, *15*(6),
682 e0034624.
683 5. Bochner, B. R., Gadzinski, P., & Panomitros, E. (2001). Phenotype microarrays for high-
684 throughput phenotypic testing and assay of gene function. *Genome Research*, *11*(7), 1246–
685 1255.
686 6. Borezée-Durant, E., Hiron, A., Piard, J.-C., & Juillard, V. (2009). Dual role of the oligopeptide
687 permease Opp3 during growth of Staphylococcus aureus in milk. *Applied and Environmental*
688 *Microbiology*, *75*(10), 3355–3357.
689 7. Bose, J. L., Fey, P. D., & Bayles, K. W. (2013). Genetic tools to enhance the study of gene
690 function and regulation in Staphylococcus aureus. *Applied and Environmental Microbiology*,
691 *79*(7), 2218–2224.
692 8. Coulter, S. N., Schwan, W. R., Ng, E. Y., Langhorne, M. H., Ritchie, H. D., Westbrock-Wadman,
693 S., Hufnagle, W. O., Folger, K. R., Bayer, A. S., & Stover, C. K. (1998). Staphylococcus aureus
694 genetic loci impacting growth and survival in multiple infection environments. *Molecular*
695 *Microbiology*, *30*(2), 393–404.

696 9. Cui, C.-Y., Li, B., & Su, X.-C. (2023). Real-time monitoring of the level and activity of
697 intracellular glutathione in live cells at atomic resolution by 19F-NMR. *ACS Central Science*,
698 *9*(8), 1623–1632.
699 10. Dasgupta, A., Sureka, K., Mitra, D., Saha, B., Sanyal, S., Das, A. K., Chakrabarti, P., Jackson,
700 M., Gicquel, B., Kundu, M., & Basu, J. (2010). An oligopeptide transporter of Mycobacterium
701 tuberculosis regulates cytokine release and apoptosis of infected macrophages. *PloS One*,
702 *5*(8), e12225.
703 11. Detmers, F. J., Lanfermeijer, F. C., Abele, R., Jack, R. W., Tampe, R., Konings, W. N., &
704 Poolman, B. (2000). Combinatorial peptide libraries reveal the ligand-binding mechanism of
705 the oligopeptide receptor OppA of Lactococcus lactis. *Proceedings of the National Academy*
706 *of Sciences of the United States of America*, *97*(23), 12487–12492.
707 12. Doeven, M. K., Abele, R., Tampé, R., & Poolman, B. (2004). The binding specificity of OppA
708 determines the selectivity of the oligopeptide ATP-binding cassette transporter. *The Journal*
709 *of Biological Chemistry*, *279*(31), 32301–32307.
710 13. Drew, D., Lerch, M., Kunji, E., Slotboom, D.-J., & de Gier, J.-W. (2006). Optimization of
711 membrane protein overexpression and purification using GFP fusions. *Nature Methods*, *3*(4),
712 303–313.
713 14. Dubois, T., Lemy, C., Perchat, S., & Lereclus, D. (2019). The signaling peptide NprX controlling
714 sporulation and necrotrophism is imported into Bacillus thuringiensis by two oligopeptide
715 permease systems. *Molecular Microbiology*, *112*(1), 219–232.
716 15. Fey, P. D., Endres, J. L., Yajjala, V. K., Widhelm, T. J., Boissy, R. J., Bose, J. L., & Bayles, K. W.
717 (2013). A genetic resource for rapid and comprehensive phenotype screening of
718 nonessential Staphylococcus aureus genes. *MBio*, *4*(1), e00537-12.
719 16. Flannagan, R. S., Heit, B., & Heinrichs, D. E. (2016). Intracellular replication of Staphylococcus
720 aureus in mature phagolysosomes in macrophages precedes host cell death, and bacterial
721 escape and dissemination. *Cellular Microbiology*, *18*(4), 514–535.

722 17. Freiberg, J. A., Reyes Ruiz, V. M., Gimza, B. D., Murdoch, C. C., Green, E. R., Curry, J. M.,
723 Cassat, J. E., & Skaar, E. P. (2024). Restriction of arginine induces antibiotic tolerance in
724 Staphylococcus aureus. *Nature Communications*, *15*(1), 6734.
725 18. Garai, P., Chandra, K., & Chakravortty, D. (2017). Bacterial peptide transporters: Messengers
726 of nutrition to virulence. *Virulence*, *8*(3), 297–309.
727 19. Grkovic, S., Brown, M. H., Hardie, K. M., Firth, N., & Skurray, R. A. (2003). Stable low-copy-
728 number Staphylococcus aureus shuttle vectors. *Microbiology*, *149*(Pt 3), 785–794.
729 20. Halsey, C. R., Lei, S., Wax, J. K., Lehman, M. K., Nuxoll, A. S., Steinke, L., Sadykov, M., Powers,
730 R., & Fey, P. D. (2017). Amino acid catabolism in staphylococcus aureus and the function of
731 carbon catabolite repression. *MBio*, *8*(1).
732 21. Handke, L. D., Gribenko, A. V., Timofeyeva, Y., Scully, I. L., & Anderson, A. S. (2018). MntC-
733 dependent manganese transport is essential for staphylococcus aureus oxidative stress
734 resistance and virulence. *MSphere*, *3*(4).
735 22. Hansen, R. E., Roth, D., & Winther, J. R. (2009). Quantifying the global cellular thiol-disulfide
736 status. *Proceedings of the National Academy of Sciences of the United States of America*,
737 *106*(2), 422–427.
738 23. Hebbeln, P., & Eitinger, T. (2004). Heterologous production and characterization of bacterial
739 nickel/cobalt permeases. *FEMS Microbiology Letters*, *230*(1), 129–135.
740 24. Hiron, A., Borezée-Durant, E., Piard, J.-C., & Juillard, V. (2007). Only one of four oligopeptide
741 transport systems mediates nitrogen nutrition in Staphylococcus aureus. *Journal of*
742 *Bacteriology*, *189*(14), 5119–5129.
743 25. Hughes, A. M., Darby, J. F., Dodson, E. J., Wilson, S. J., Turkenburg, J. P., Thomas, G. H., &
744 Wilkinson, A. J. (2022). Peptide transport in Bacillus subtilis - structure and specificity in the
745 extracellular solute binding proteins OppA and DppE. *Microbiology*, *168*(12).
746 26. Hussain, M., Hastings, J. G., & White, P. J. (1991). A chemically defined medium for slime
747 production by coagulase-negative staphylococci. *Journal of Medical Microbiology*, *34*(3),

748 143–147.

749 27. Jeong, B., Shah, M. A., Roh, E., Kim, K., Park, I., & Bae, T. (2022). Staphylococcus aureus does
750 not synthesize arginine from proline under physiological conditions. *Journal of Bacteriology*,
751 *204*(6), e0001822.

752 28. Kotov, V., Killer, M., Jungnickel, K. E. J., Lei, J., Finocchio, G., Steinke, J., Bartels, K., Strauss, J.,
753 Dupeux, F., Humm, A.-S., Cornaciu, I., Márquez, J. A., Pardon, E., Steyaert, J., & Löw, C.
754 (2023). Plasticity of the binding pocket in peptide transporters underpins promiscuous
755 substrate recognition. *Cell Reports*, *42*(8), 112831.

756 29. Kubica, M., Guzik, K., Koziel, J., Zarebski, M., Richter, W., Gajkowska, B., Golda, A., Maciag-
757 Gudowska, A., Brix, K., Shaw, L., Foster, T., & Potempa, J. (2008). A potential new pathway
758 for staphylococcus aureus dissemination: The silent survival of S. aureus phagocytosed by
759 human monocyte-derived macrophages. *PloS One*, *3*(1), e1409.

760 30. Lehman, M. K., Nuxoll, A. S., Yamada, K. J., Kielian, T., Carson, S. D., & Fey, P. D. (2019).
761 Protease-mediated growth of Staphylococcus aureus on host proteins is opp3 dependent.
762 *MBio*, *10*(2).

763 31. Lehman, M. K., Sturd, N. A., Razvi, F., Wellems, D. L., Carson, S. D., & Fey, P. D. (2023).
764 Proline transporters ProT and PutP are required for Staphylococcus aureus infection. *PLoS*
765 *Pathogens*, *19*(1), e1011098.

766 32. Lensmire, J. M., Dodson, J. P., Hsueh, B. Y., Wischer, M. R., Delekta, P. C., Shook, J. C.,
767 Ottosen, E. N., Kies, P. J., Ravi, J., & Hammer, N. D. (2020). The staphylococcus aureus cystine
768 transporters TcyABC and TcyP facilitate nutrient sulfur acquisition during infection. *Infection*
769 *and Immunity*, *88*(3).

770 33. Lensmire, J. M., Wischer, M. R., Kraemer-Zimpel, C., Kies, P. J., Sosinski, L., Ensink, E.,
771 Dodson, J. P., Shook, J. C., Delekta, P. C., Cooper, C. C., Havlichek, D. H., Jr, Mulks, M. H.,
772 Lunt, S. Y., Ravi, J., & Hammer, N. D. (2023). The glutathione import system satisfies the
773 Staphylococcus aureus nutrient sulfur requirement and promotes interspecies competition.

774 *PLoS Genetics*, *19*(7), e1010834.

775 34. Li, C., Yue, Z., Newstead, S., & Voth, G. A. (2022). Proton coupling and the multiscale kinetic
776 mechanism of a peptide transporter. *Biophysical Journal*, *121*(12), 2266–2278.

777 35. Lichtinger, S. M., Parker, J. L., Newstead, S., & Biggin, P. C. (2024). The mechanism of
778 mammalian proton-coupled peptide transporters. *ELife*, *13*.

779 36. Lushchak, V. I. (2012). Glutathione homeostasis and functions: potential targets for medical
780 interventions. *Journal of Amino Acids*, *2012*, 736837.

781 37. Lyons, J. A., Parker, J. L., Solcan, N., Brinth, A., Li, D., Shah, S. T. A., Caffrey, M., & Newstead,
782 S. (2014). Structural basis for polyspecificity in the POT family of proton-coupled
783 oligopeptide transporters. *EMBO Reports*, *15*(8), 886–893.

784 38. Maqbool, A., Levdikov, V. M., Blagova, E. V., Hervé, M., Horler, R. S. P., Wilkinson, A. J., &
785 Thomas, G. H. (2011). Compensating stereochemical changes allow murein tripeptide to be
786 accommodated in a conventional peptide-binding protein. *The Journal of Biological*
787 *Chemistry*, *286*(36), 31512–31521.

788 39. McInnes, L., Healy, J., & Melville, J. (2018). UMAP: Uniform Manifold Approximation and
789 Projection for Dimension Reduction. *ArXiv [Stat.ML]*. arXiv. http://arxiv.org/abs/1802.03426

790 40. Meister, A. (1988). Glutathione metabolism and its selective modification. *The Journal of*
791 *Biological Chemistry*, *263*(33), 17205–17208.

792 41. Minhas, G. S., Bawdon, D., Herman, R., Rudden, M., Stone, A. P., James, A. G., Thomas, G. H.,
793 & Newstead, S. (2018). Structural basis of malodour precursor transport in the human axilla.
794 *ELife*, *7*.

795 42. Miroux, B., & Walker, J. E. (1996). Over-production of proteins in Escherichia coli: mutant
796 hosts that allow synthesis of some membrane proteins and globular proteins at high levels.
797 *Journal of Molecular Biology*, *260*(3), 289–298.

798 43. Nasher, F., Heller, M., & Hathaway, L. J. (2018). Streptococcus pneumoniae Proteins AmiA,
799 AliA, and AliB Bind Peptides Found in Ribosomal Proteins of Other Bacterial Species.

Frontiers in Microbiology, *8*.

44. Park, J. T., Raychaudhuri, D., Li, H., Normark, S., & Mengin-Lecreulx, D. (1998). MppA, a periplasmic binding protein essential for import of the bacterial cell wall peptide L-alanyl-gamma-D-glutamyl-meso-diaminopimelate. *Journal of Bacteriology*, *180*(5), 1215–1223.

45. Parker, J. L., Mindell, J. A., & Newstead, S. (2014). Thermodynamic evidence for a dual transport mechanism in a POT peptide transporter. *ELife*, *3*. https://doi.org/10.7554/elife.04273

46. Parra-Lopez, C., Baer, M. T., & Groisman, E. A. (1993). Molecular genetic analysis of a locus required for resistance to antimicrobial peptides in Salmonella typhimurium. *EMBO J.*, *12*(11), 4053–4062.

47. Pletzer, D., Lafon, C., Braun, Y., Köhler, T., Page, M. G. P., Mourez, M., & Weingart, H. (2014). High-throughput screening of dipeptide utilization mediated by the ABC transporter DppBCDF and its substrate-binding proteins DppA1-A5 in Pseudomonas aeruginosa. *PloS One*, *9*(10), e111311.

48. Remy, L., Carrière, M., Derré-Bobillot, A., Martini, C., Sanguinetti, M., & Borezée-Durant, E. (2013). The Staphylococcus aureus Opp1 ABC transporter imports nickel and cobalt in zinc-depleted conditions and contributes to virulence. *Molecular Microbiology*, *87*(4), 730–743.

49. Reslane, I., Halsey, C. R., Stastny, A., Cabrera, B. J., Ahn, J., Shinde, D., Galac, M. R., Sladek, M. F., Razvi, F., Lehman, M. K., Bayles, K. W., Thomas, V. C., Handke, L. D., & Fey, P. D. (2022). Catabolic ornithine carbamoyltransferase activity facilitates growth of Staphylococcus aureus in defined medium lacking glucose and arginine. *MBio*, *13*(3), e0039522.

50. Rivera, K. G., Tanaka, K. J., Buechel, E. R., Origel, O., Jr, Harrison, A., Mason, K. M., & Pinkett, H. W. (2024). Antimicrobial peptide recognition motif of the substrate binding protein SapA from nontypeable Haemophilus influenzae. *Biochemistry*, *63*(3), 294–311.

51. Samsudin, F., Parker, J. L., Sansom, M. S. P., Newstead, S., & Fowler, P. W. (2016). Accurate

826 prediction of ligand affinities for a proton-dependent oligopeptide transporter. *Cell Chemical*
827 *Biology*, *23*(2), 299–309.
828 52. Shaw, L., Golonka, E., Potempa, J., & Foster, S. J. (2004). The role and regulation of the
829 extracellular proteases of Staphylococcus aureus. *Microbiology*, *150*(Pt 1), 217–228.
830 53. Shibamura-Fujiogi, M., Wang, X., Maisat, W., Koutsogiannaki, S., Li, Y., Chen, Y., Lee, J. C., &
831 Yuki, K. (2022). GltS regulates biofilm formation in methicillin-resistant Staphylococcus
832 aureus. *Communications Biology*, *5*(1), 1284.
833 54. Shull, L. M., Wolter, D. J., Kunkle, D. E., Legg, K. A., Giedroc, D. P., Skaar, E. P., Hoffman, L. R.,
834 & Reniere, M. L. (2024). Analysis of genetic requirements and nutrient availability for
835 Staphylococcus aureus growth in cystic fibrosis sputum. *BioRxiv.Org: The Preprint Server for*
836 *Biology*.
837 55. Simpson, B. W., Gilmore, M. C., McLean, A. B., Cava, F., & Trent, M. S. (2023). Escherichia coli
838 utilizes multiple peptidoglycan recycling permeases with distinct strategies of recycling.
839 *Proceedings of the National Academy of Sciences of the United States of America*, *120*(44),
840 e2308940120.
841 56. Slamti, L., & Lereclus, D. (2019). The oligopeptide ABC-importers are essential
842 communication channels in Gram-positive bacteria. *Research in Microbiology*, *170*(8), 338–
843 344.
844 57. Smith, M. W., Tyreman, D. R., Payne, G. M., Marshall, N. J., & Payne, J. W. (1999). Substrate
845 specificity of the periplasmic dipeptide-binding protein from Escherichia coli: experimental
846 basis for the design of peptide prodrugs. *Microbiology*, *145 (Pt 10)*(10), 2891–2901.
847 58. Solcan, N., Kwok, J., Fowler, P. W., Cameron, A. D., Drew, D., Iwata, S., & Newstead, S.
848 (2012). Alternating access mechanism in the POT family of oligopeptide transporters:
849 Alternating access mechanism in the POT family. *The EMBO Journal*, *31*(16), 3411–3421.
850 59. Sprouffske, K., & Wagner, A. (2016). Growthcurver: an R package for obtaining interpretable
851 metrics from microbial growth curves. *BMC Bioinformatics*, *17*(1), 172.

852 60. Tong, S. Y. C., Davis, J. S., Eichenberger, E., Holland, T. L., & Fowler, V. G., Jr. (2015).
853 Staphylococcus aureus infections: epidemiology, pathophysiology, clinical manifestations,
854 and management. *Clinical Microbiology Reviews*, *28*(3), 603–661.
855 61. Urso, A., Monk, I. R., Cheng, Y.-T., Predella, C., Wong Fok Lung, T., Theiller, E. M., Boylan, J.,
856 Perelman, S., Baskota, S. U., Moustafa, A. M., Lohia, G., Lewis, I. A., Howden, B. P., Stinear, T.
857 P., Dorrello, N. V., Torres, V., & Prince, A. S. (2024). Staphylococcus aureus adapts to exploit
858 collagen-derived proline during chronic infection. *Nature Microbiology*, *9*(10), 2506–2521.
859 62. Wang, Z., Bie, P., Cheng, J., Lu, L., Cui, B., & Wu, Q. (2016). The ABC transporter YejABEF is
860 required for resistance to antimicrobial peptides and the virulence of Brucella melitensis.
861 *Scientific Reports*, *6*, 31876.
862 63. Yu, D., Pi, B., Yu, M., Wang, Y., Ruan, Z., Feng, Y., & Yu, Y. (2014). Diversity and evolution of
863 oligopeptide permease systems in staphylococcal species. *Genomics*, *104*(1), 8–13.
864 64. Zeden, M. S., Kviatkovski, I., Schuster, C. F., Thomas, V. C., Fey, P. D., & Gründling, A. (2020).
865 Identification of the main glutamine and glutamate transporters in Staphylococcus aureus
866 and their impact on c-di-AMP production. *Molecular Microbiology*, *113*(6), 1085–1100.
867 65. Zheng, F., Shao, Z.-Q., Hao, X., Wu, Q., Li, C., Hou, H., Hu, D., Wang, C., & Pan, X. (2018).
868 Identification of oligopeptide-binding protein (OppA) and its role in the virulence of
869 Streptococcus suis serotype 2. *Microbial Pathogenesis*, *118*, 322–329.
870